Experimental and simulation study on the influence of sand on heat dissipation performance of special vehicle radiator

Yong Gui[1,*], *Liang* Zhou[2], *Qianqian* Zhang[2], *Hongbin* Liu[1], and *Qingguo* Luo[1]

[1]Department of vehicle Engineering, Academy of Armored Forces, Beijing 100072, PR China
[2]Army Equipment Project Management Center, Beijing 100072, PR China

Abstract. The radiator of special vehicle often exposed to sand condition, and the sand have great influence on the performance of radiator, in order to figure out the impact, the physical model of a radiator is built, the three-dimensional numerical simulation of the gas and water flow field of the radiator is carried out by adopting discrete phase model (DPM) as well as the SIMPLE scheme. Then, the relationship between different factors (such as air velocity, sand particle size, sand concentration) and heat transfer coefficient are obtained by means of simulation, which provides a basis for the optimization design of the special vehicle radiator. A test bench is built, and the simulation is verified to be correct by comparing the simulation result with the test result.

Keywords: Sand, Special vehicle, Heat dissipation performance, Gas-solid two-phase flow.

1 Introduction

Radiator is an important part in the cooling system of special vehicle, the heat-sinking capability of the radiator is significant to the vehicle engine [1-2]. Arid climate, poor rainfall often appeared in plateau area of China, and the heat-sinking capability of special vehicle radiator is serious affected by the gas-sand two phase flow, which is generated when special vehicle cross those area[3]. In order to promote special vehicle's environment adaptivity and battleground viability, the influence of sand condition on the heat-sinking capability of radiator needs to be studied.

Few such literatures can be found because automobile seldom exposed in sand condition. However, the radiating process of radiator in sand condition is belong to the domain of gas-solid two-phase flow, which has been researched in the areas of airspace engine[4-5], reclaiming of residual heat[6], new energy resources[7], fluid bed[8-12], pulverized coal fired boiler[13-14] and so on.

A radiator of a special vehicle is taken as the research object in this paper. The geometry parameter model of the radiator is established based on Fluent numerical stimulation software, and the discrete phase model and interphase coupling SIMPLEC

* Corresponding author: gy8144@163.com

algorithm are applied to the three-dimensional numerical simulation calculation of gas side and water side flow fields of the radiator. A test bed of the heat transfer performance of radiators in sand environment is established, and the performance test is carries out based on orthographic design method, and in accordance with the relevant national standards, the ranges of composition, particle size, concentration and other factors of sand is determined. The stimulation model is verified to be correct by comparing the simulation data with experimental data, Based on the stimulation model, the trajectory of sand particles and the mechanism of sand affection on heat dissipation are analyzed, furthermore, the influence of air velocity, sand particle size, and sand concentration on heat transfer is studied, which provides the basis for the optimal design of special vehicle radiators.

2. Simulation analysis

2.1 Theoretical model

Euler-Lagrange is the usually used method for the study of gas-solid two-phase flow. Based on different properties of media, the Euler-Lagrange method regards the gas phase as continuous phase, and the solid phase as discrete phase. The governing equations are respectively

2.1.1 Control equation for continuous phase

Continuity equation

$$\frac{\partial u_i}{\partial x_i} = 0 \tag{1}$$

Momentum equation

$$\rho u_j \frac{\partial u_i}{\partial x_j} = -\frac{\partial p}{\partial x_i} + \mu \frac{\partial^2 u_i}{\partial x_i \partial x_j} + \frac{\partial}{\partial x_j}(-\overline{\rho u_j' \rho u_i'}) + \rho g \beta (T - T_{ref}) + S_i \tag{2}$$

Energy equation

$$\frac{\partial \rho u_j T}{\partial x_i} = \frac{\partial}{\partial x_j}\left[\left(\frac{k}{c_p} + \frac{u_t}{\sigma_T}\right)\frac{\partial T}{\partial x_j}\right] \tag{3}$$

$k-\varepsilon$ Turbulence equation

$$\frac{\partial(\rho k)}{\partial t} + \frac{\partial(\rho k \mu_i)}{\partial x_i} = \frac{\partial}{\partial x_j}\left[\left(\mu + \frac{\mu_t}{\sigma_k}\right)\frac{\partial k}{\partial x_j}\right] + G_k + G_b - \rho\varepsilon - Y_M + S_k \tag{4}$$

Diffusion equation

$$\frac{\partial(\rho\varepsilon)}{\partial t} + \frac{\partial(\rho\varepsilon\mu_i)}{\partial x_i} = \frac{\partial}{\partial x_j}\left[\left(\mu + \frac{\mu_t}{\sigma_\varepsilon}\right)\frac{\partial \varepsilon}{\partial x_j}\right] + \frac{C_{1\varepsilon}\varepsilon}{k}(G_k + C_{3\varepsilon}G_b) - C_{2\varepsilon}\rho\frac{\varepsilon^2}{k} + S_\varepsilon \tag{5}$$

In the equations, ρ, T, u, u', c_p are the density, temperature, speed, pulsation velocity and specific heat capacity at constant pressure of the fluid respectively. μ and μ_t are the dynamic viscosity coefficient and turbulent viscosity coefficient of the fluid, T_{ref} refers to environment temperature, β is the thermal expansion coefficient, k is the turbulence energy, ε is the turbulent dissipation rate, S_i is the loss of momentum in porous media, $C_{1\varepsilon}$, $C_{2\varepsilon}$, C_μ, δ_κ and δ_ε are empirical constants, G_k and G_b are the average

velocity gradient and the generation terms of the turbulence energy κ respectively. The indicator range of i and j is 1, 2, 3.

2.1.2 Discrete phase control equation

Equilibrium equation

$$\frac{du_p}{dt} = F_D\left(u - u_p\right) + \frac{u_p\left(\rho_p - \rho\right)}{\rho_p} + F_x \tag{6}$$

In the equation, $F_D\left(u - u_p\right)$ is the drag force of a unit mass of particles.

$$F_D = \frac{18\mu}{\rho_p d_p^2}\frac{C_D \mathrm{Re}_p}{24} \tag{7}$$

$$F_X = \frac{pd}{2\rho_p dt}(u - u_p) \tag{8}$$

u is the speed of fluid, u_p is the speed of particles, ρ_p is the density of particles, d_p is the particle size of particles, F_x is the additional mass force [10], Re_p is the Reynolds number of particle, which is defined as

$$\mathrm{Re}_p = \frac{\rho d_p \left|u_p - u\right|}{\mu} \tag{9}$$

The expression of drag coefficient C_D is

$$C_D = a_1 + \frac{a_2}{\mathrm{Re}} + \frac{a_3}{\mathrm{Re}} \tag{10}$$

For spherical particles, when the Reynolds number is within a certain range, a_1, a_2, and a_3 are constants.

Stochastic trajectory model, random walk model and particle cloud model are three common particle orbit tracking models in FLUENT, Among them, the stochastic trajectory model can consider not only the influences of air flow, turbulence, pulsation and fluency when solid particles are moving, but also the randomness of their moving directions, so the stochastic trajectory model can simulate the actual particles motion of two-phase flow well.

2.2 Physical model

2.2.1 Three-dimensional solid model

The plate-fin radiator structure is mainly composed of gas side, water side rectangular fins and partitions.

Due to the complex structure of the plate-fin radiator, the number of generated meshes will be very large, and the requirements for computer hardware and calculation time will be very high, even unbearable. In order to save computing resources, the basic unit of plate-fin radiator is taken as the research object for numerical calculation in the study. The three-dimensional solid model is shown in Fig.1.

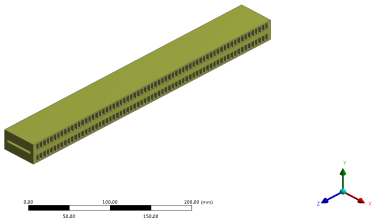

Fig. 1. Three-dimensional model of the radiator basic unit.

2.2.2 Fluid domain model building and meshing

Gas-side and water-side fluid domain models are established respectively. In order to fully develop the fluid flow and prevent the outlet from generating backflow, the distance from air inlet & outlet to the radiator as three times to six times the height of radiator when the gas-side fluid domain model is established,, as shown in Fig. 2.

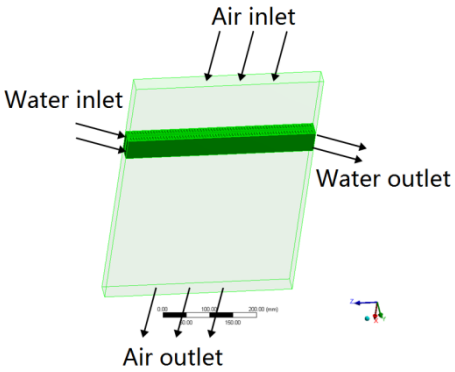

Fig. 2. Fluid domain model.

2.3 Simulation analysis

2.3.1 Influence of different flow speeds on heat transfer

The variation curve of the wind side heat transfer coefficient with the flow speed is shown in Fig. 3. The gas side heat transfer coefficient goes up as the flow speed increases. As the flow speed increases, the collision frequency between sand particles and the wall increases and the stay time decreases. As the damage effect on the boundary layer enhancing, the increase in air volume may also reduce the thickness of boundary layer and increase the heat transfer coefficient of pure gas stream, which enhances the overall heat transfer effect on the gas side.

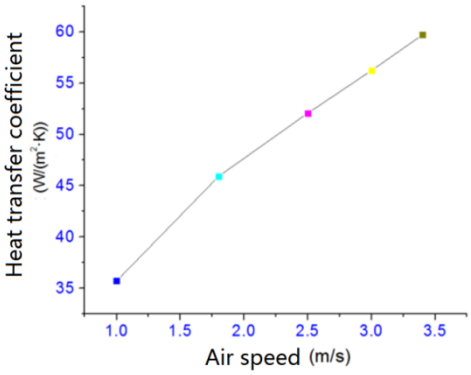

Fig. 3. Effect of air speed on heat transfer coefficient.

2.3.2 Effect of different particle size on heat transfer

The variation curve of the wind side heat transfer coefficient with the particle size is shown in Fig. 4. The gas side heat transfer coefficient reduces as particle size increases. As the particle size increases, the number of particles that contact and collide with the heat transfer surface per unit time decreases, and thus reducing the damage effect on the boundary layer of the heat transfer surface, which reduces the heat transfer effect.

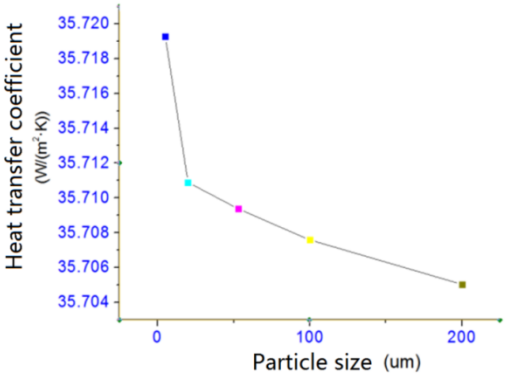

Fig. 4. Effect of particle size on heat transfer coefficient.

2.3.3 Effect of different concentrations on heat transfer

The variation curve of the wind side heat transfer coefficient with the concentration is shown in Fig. 5. The gas side heat transfer coefficient increases as the sand particle concentration increases. As the volume fraction of sand particles increases, the proportion of particles in the gas-solid two-phase flow increases correspondingly, increasing the probability of contact and collision between particles and the heat transfer surface, and enhancing the damage effect on the boundary layer of heat transfer surface, which improves the heat transfer effect.

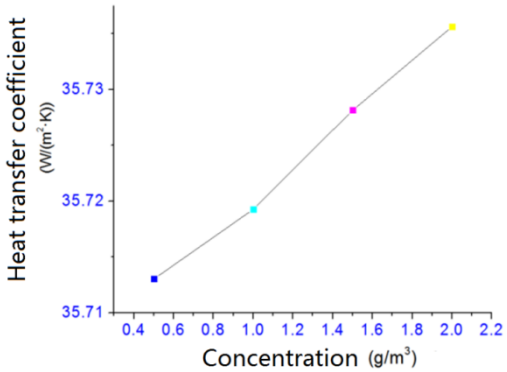

Fig. 5. Effect of coefficient on heat transfer coefficient.

3 Experimental study

A test bench of the heat transfer performance of the radiator in sand environment is established. Based on the orthographic design method, a bed test plan is designed, and the performance test is carried out, which helps verify the stimulation model of radiator performance.

3.1 Working principle

The test bench includes three parts: oil-water side, wind side, and data acquisition and control side. It is mainly composed of heat-conducting oil boiler, oil pump, electric control valve, heat exchanger, water pump, radiator, feeder, fan, wind speed air flow meter, temperature sensor, data collector, computer and other components. Each part work is as follows:

(1) Oil-water side: the main function of the oil-water side is to warm the water of the radiator. The oil is pumped into the oil boiler by oil pump for heating, and then flows into the heat exchanger, in which exchange heat is conducted between the oil and the water. The oil flow in the oil line is tested by Flow Meter 1 and the water flow in the waterway is detected by Flow Meter 2. The temperatures of oil at the inlet and outlet of the heat exchanger are detected through Temperature Sensor 1 and Temperature Sensor 2 respectively. The temperatures of water at the inlet and outlet of the heat exchanger are detected by Temperature Sensor 3 and Temperature Sensor 4 respectively. The above signals are all fed back to the computer by data collector. The oil pump speed and the electric control valve opening are controlled by computer through the controller, in order to adjust the oil temperature in the oil line, and thereby control the water temperature within a reasonable range, as shown in Fig. 6.

(2) Gas side: cooling air enters the air passage from the air inlet, mixed with the sand which sent by the feeder, the air will thoroughly mix with sand when passes through the uniform mixing section. Then, under the action of the fan, the mixed air will cool the water in the radiator when passing through the radiator, and finally discharged from the sand outlet. The temperatures of air at the inlet and outlet of the radiator are detected by Temperature Sensor 1 and Temperature Sensor 2 respectively and the temperatures of water at the inlet and outlet of the radiator are detected by Temperature Sensor 3 and Temperature Sensor 4 respectively. The wind speed at the inlet and outlet of the radiator are tested by Wind Speed Sensor 1 and Wind Speed Sensor 2 respectively. The above signals are sent to the computer through the data collector. The computer controls the feeding amount of the

feeder through the controller for simulating different sand concentrations, and controls the fan speed through the controller for stimulating different wind speeds, as shown in Fig. 7.

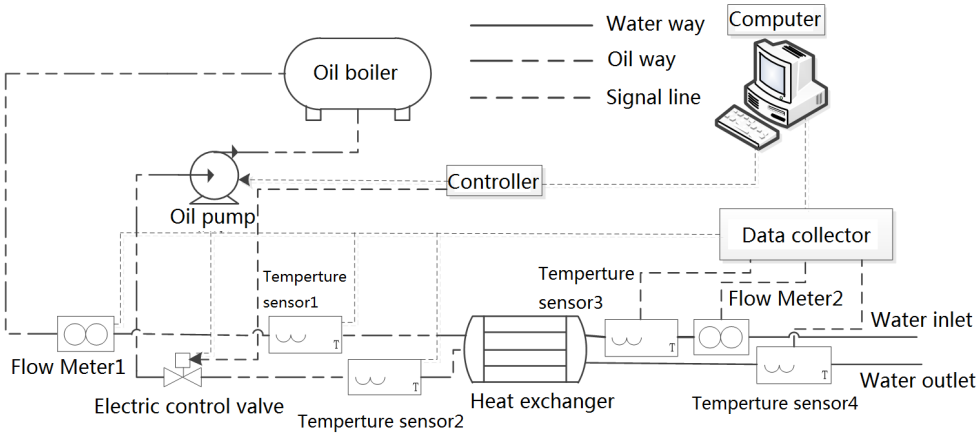

Fig. 6. The working sketch of oil-water side.

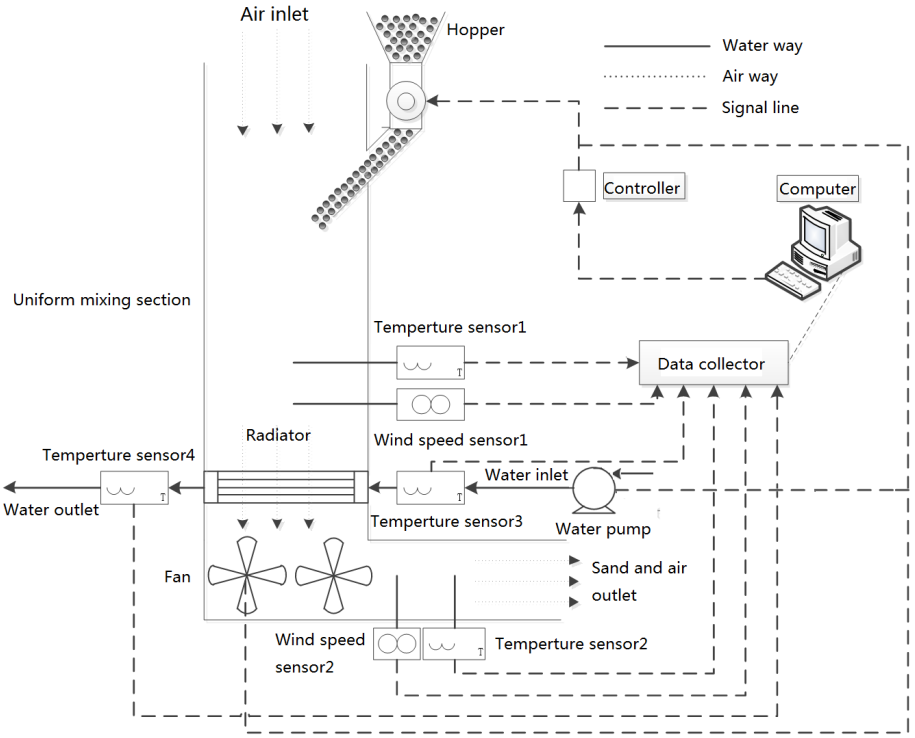

Fig. 7. The working sketch of air side.

(3) Data acquisition and control side: The data acquisition and control side need to collect the relevant temperature as well as water and air flow on the oil-water side and wind side, and control parameters such as fan speed, oil pump speed, water pump speed, feeding amount of the feeder, and the electric control valve opening.

3.2 Test bench

The test bench is shown in Fig. 8. The rated power of the oil boiler is 80KW. The heat exchanger is a finned heat exchanger with high efficiency. The electric control valve is flange-mounted, with 1% adjustment precision. All pumps are driven by variable frequency motors, which controlled by the frequency converters.

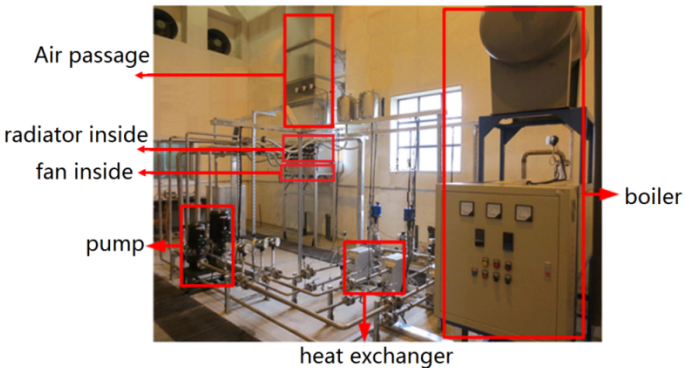

Fig. 8. The test bench.

3.3 Test and analysis

The atmospheric pressure is 0.101Mpa and the temperature is 24°C. The inlet water flow of the radiator is 2.42 m^3/h and the temperature is 90°C. When the fan speeds are 1,000r/min, 1,500r/min, 2,000r/min, and 2,500r/min, the wind speeds of windward surface of the radiator are measured as 1.0m/s, 1.8m/s, 2.5m/s and 3.4m/s respectively.

Four typical sand particle sizes of 5um, 20um, 53um and 200um are selected, with the sand concentrations of $0.5g/m^3$, $1.0g/m^3$, $1.5g/m^3$ and $2.0g/m^3$ respectively. The orthographic design method is used in the test.

In the simulation, the inlet condition of the radiator is set to be consistent with the heat transfer performance test of each group, and the outlet temperature of the radiator is used as the model correctness comparison parameter. Tab.1 is the comparison between the simulation calculation and test bench result of the outlet temperature of the radiator, with the maximum relative deviation of 7.43%. It can be seen that the simulation model is accurate and reliable.

Table 1. Comparison of error between simulation and measured data.

Number	Test air outlet temperature /℃	simulation air outlet temperature /℃	Errors /%
1	55.8	52.6	5.85
2	55.6	52.4	5.68
3	55.5	52.3	5.79
4	55.2	51.9	5.97
5	53.7	50.1	6.55
6	53.4	50.0	6.27
7	52.4	49.1	6.36
8	52.6	49.4	6.13
9	51.5	47.9	7.11
10	50.9	47.2	7.43
11	51.6	48.4	6.25
12	51.3	48.1	6.31

13	49.5	47.0	4.99
14	48.8	46.7	4.2
15	49.2	47.2	4.08
16	49.9	47.8	4.05

4 Conclusions

By combining test with simulation, the trajectory of sand particles is studied, the mechanism of sand affecting heat transfer is analyzed, the influences of air flow speed, sand particle size, sand concentration on the heat transfer performance of special vehicle radiators are studied in this paper, and thus, A basis for the optimal design of special vehicle radiators is provided in this study.

References

1. G.A. Oliveira, E.M.C. Contreras, E.P.B Filho. Experimental study on the heat transfer of MWCNT water nanofluid flowing in a car radiator, Applied Thermal Engineering. 111(2017)1450-1456.
2. K.Y. Leong, R. Saidur, S.N. Kazi, etal. Performance investigation of an automotive car radiator operated with nanofluid-based coolants. Applied Thermal Engineering. 30(2010)17-18.
3. J.S Feng, H. Dong, J.Y Gao, etal. Numerical investigation of gas-solid heat transfer process in vertical tank for sinter waste heat recovery. Applied Thermal Engineering. 107 (2016) 135-143.
4. R. Madabhushi, J. Sabnis, F. Jong, et al. Calculation of the Two-Phase Aft-Dome Flow Field in Solid Rocket Motors.Journal of Propulsion. 2 (1991)178-184.
5. M. Golafshani, H. T. Loh. Computation of Two-Phase Viscous Flow in Solid Rocket Motors Using a Flux-Split Eulerian Larangian Technique. AIAA 89-2785.
6. F. Pitie, C.Y. Zhao, J. Baeyens, etal. Circulating fluidized bed heat recovery/storage and its potential to use coated phase-change-material (PCM) particles. Applied Energy. 109 (2013) 505-513.
7. G. Flamant, H. Benoit, J. Sans. Dense suspension of solid particles as a new heat transfer fluid for concentrated solar thermal plants: on-sun proof of concept. Chemical Engineering Science. 102(2013) 567-576.
8. R. Pešić, T.K. Radoičić, N. Bošković-Vragolović. Heat transfer between a packed bed and a larger immersed spherical particle. Int. J. Heat Mass Tran. 78 (2014)130-136.
9. A. Singhal, S. Cloete, S. Radl, etal. Heat transfer to a gas from densely packed beds of monodisperse spherical particles. Chemical Engineering Journal. 314 (2017) 27-37.
10. H. Wu, N. Gui, X.T. Yang, etal. Numerical simulation of heat transfer in packed pebble beds: CFD-DEM coupled with particle thermal radiation. International Journal of Heat and Mass Transfer. 110(2017)393-405.
11. H.G. Wang, G.Z. Qiu, J.M. Ye, etal. Experimental study and modelling on gas–solid flow in a lab-scale fluidised bed with Wurster tube. Powder Technology. 300 (2016) 14-27.
12. H. Wahyudi, K.W Chu, A.B Yu. 3D particle-scale modeling of gas–solids flow and heat transfer in fluidized beds with an immersed tube. International Journal of Heat and Mass Transfer 97 (2016) 521-537.

13. S. Chakraborty, A. Rajora, S.P. Singh, etal. Heat transfer and discrete phase modelling of coal combustion in a pusher type reheating furnace. Applied Thermal Engineering. 116(2017) 66-78.
14. X.Y. Guan, S.Z. Sun, Y.Z Guo, etal. Experimental Study on the Gas-Solid Two Phase Flow and Numerical Prediction of the Blade Surface Erosion in a Louver Coal Concentrator. Science Technology and Engineering. 33(2010) 8131-8237.